



Published in final edited form as:

*Pain Med.* 2015 November ; 16(11): 2121–2133. doi:10.1111/pme.12785.

## The Subjective Experience of Pain: an FMRI Study of Percept-related Models and Functional Connectivity

Claire E. Wilcox<sup>1</sup>, Andrew R. Mayer<sup>2,3</sup>, Terri M. Teshiba<sup>2</sup>, Josef Ling<sup>2</sup>, Bruce W. Smith<sup>4</sup>, George L. Wilcox<sup>5</sup>, and Paul G. Mullins<sup>6</sup>

<sup>1</sup>The University of New Mexico Department of Psychiatry

<sup>2</sup>The Mind Research Network, Albuquerque, NM 87106, USA

<sup>3</sup>Neurology Department, University of New Mexico School of Medicine, Albuquerque, NM 87131, USA

<sup>4</sup>Psychology Department, University of New Mexico, Albuquerque, NM 87131, USA

<sup>5</sup>Departments of Neuroscience, Pharmacology and Dermatology, University of Minnesota, Minneapolis, MN 55455, USA

<sup>6</sup>Bangor Imaging Center, School of Psychology, Bangor University, Gwynedd LL57 2AS, UK

### Abstract

**Objective**—Previous work suggests that the perception of pain is subjective and dependent on individual differences in physiological, emotional and cognitive states. Functional magnetic resonance imaging (fMRI) studies have utilized both stimulus-related (nociceptive properties) and percept-related (subjective experience of pain) models to identify the brain networks associated with pain. Our objective was to identify the network involved in processing subjective pain during cold stimuli.

**Methods**—The current fMRI study directly contrasted a stimulus-related model with a percept-related model during blocks of cold pain stimuli in healthy adults. Specifically, neuronal activation was modelled as a function of changes in stimulus intensity versus as a function of increasing/decreasing levels of subjective pain corresponding to changes in pain ratings. In addition, functional connectivity analyses were conducted to examine intrinsic correlations between three proposed sub-networks (sensory/discriminative, affective/motivational, and cognitive/evaluative) involved in pain processing.

**Results**—The percept-related model captured more extensive activation than the stimulus-related model and demonstrated an association between higher subjective pain and activation in expected cortical (DLPFC, VLPFC, insula, ACC extending into preSMA) and subcortical (thalamus, striatum) areas. Moreover, connectivity results supported the posited roles of dACC and insula as key relay sites during neural processing of subjective pain. In particular, anterior insula appeared

---

Corresponding author: Claire Wilcox MD; The University of New Mexico, Department of Psychiatry, 1 University of New Mexico, MSC 09-5030, Albuquerque, NM 87131; cewilcox@salud.unm.edu.

Disclosures:

The authors have no conflicts of interest to report.

to link sensory/discriminative regions with regions in the other sub-networks, and dACC appeared to serve as a hub for affective/motivational, cognitive/evaluative, and motor sub-networks.

**Conclusions**—Using a percept-related model, brain regions involved in the processing of subjective pain during the application of cold stimuli were identified. Connectivity analyses identified linkages between key sub-networks involved in processing subjective pain.

### Keywords

pain; ratings; percept-related; connectivity; FMRI

## Introduction

Functional neuroimaging studies have identified several brain regions associated with pain and the application of noxious stimuli, including the primary (S1) and secondary (S2) somatosensory cortex, anterior cingulate cortex (ACC), middle cingulate cortex (MCC), pre-SMA (supplementary motor area), SMA, anterior and posterior aspects of the insula, prefrontal cortices (PFC), the periaqueductal grey, limbic structures (amygdala, striatum), cerebellum, and thalamus (1–9). However, active debate remains regarding to what degree these different regions mediate the sensory/discriminative, affective/motivational, cognitive/evaluative, and motor components of the pain response (1, 3, 10, 11) and to what degree activation in these regions is specific to pain, or just active during many kinds (nociceptive and non-nociceptive) of phasic stimulus processing (12). One model posits that the spinothalamic ascending pain pathway projects to somatosensory cortex during initial stimulus processing, and that the ACC, MCC, medial thalamus, insula, dorsolateral prefrontal cortex (DLPFC) and temporoparietal junction play important roles in assigning salience and emotional meaning to noxious (and probably a variety of other) stimuli. Moreover, the DLPFC and ACC orchestrate top-down modulation of ascending pathways from the spinal cord. Finally, the preSMA, SMA and cerebellum orchestrate motor responses to pain (3).

Examining neuronal activation in relation to physical properties of a painful stimulus, such as intensity and/or duration (stimulus-related FMRI) is valuable (13). However, stimulus duration does not necessarily correspond that of the experienced pain (14) and sensitization/habituation is known to result in changed pain perceptions to the same stimulus over time (15–17). This lack of correspondence has led to the development of percept-related studies, where brain activity is considered in relation to the subjective and changing experience of pain as reported or recorded by the subjects themselves (2, 3, 5, 6, 13, 18–25), which has particular importance in efforts to understand mechanisms of chronic pain (3). Previous percept-related FMRI studies have used a variety of methods to measure the brain responses associated with subjective pain, including continuous ratings during stimulus presentation versus post-stimulus ratings, visual analogue scale ratings versus yes/no ratings, induced pain versus spontaneously arising pain, thermal stimuli (heat) versus chemical stimuli, and rectal mechanical distention versus other mechanical tactile stimuli (2, 3, 5, 6, 13, 18–25). However, to date, no work has parsed the brain activation associated with stimulus presentation from that associated with subjective experience of pain using a hierarchical regression model to isolate the variance associated with one from the other. In addition,

although prior work has determined the brain regions activated during application of cold stimuli (3), no studies have identified activation associated with *subjective pain during application of a cold noxious stimulus*, the pain from which is believed to have a different physiological basis from that of heat stimuli (26, 27).

The primary aim of the current study was to identify brain regions demonstrating differential functional activity related to basic noxious thermal (cold) stimulus properties (stimulus-related activation) compared to the subjective experience of pain during continuous ratings (percept-related). We predicted that activation within brain regions associated with pain in previous studies would be greater during percept-related vs. stimulus-related periods replicating previous work, with greater activation in areas theoretically involved in higher level components (cognitive/evaluative, affective/motivational) of pain processing (such as PFC, ACC, and anterior insula) (3).

Another way to further understand the brain networks involved in processing pain is to do functional connectivity analyses to quantify the degree of temporal synchrony between different brain regions (3, 28–34). In this study, as a secondary aim, we used functional connectivity analysis with seed regions derived from the percept-related fMRI findings to investigate resting connectivity within the sensory/discriminative, affective/motivational, and cognitive/evaluative networks proposed to respond to pain.

## Methods

### Subjects

Twenty-one healthy adult volunteers (9 female, 12 male) participated in the study. One female subject was identified as an outlier (above three standard deviations) on head motion parameters based on previously published algorithms (35) and was excluded from further analyses. The twenty remaining subjects (mean age = 29 +/- 6.4 years) included in the final analyses were strongly right-handed (mean Edinburgh Handedness Inventory score = 89.2% +/- 17.7%) and none reported a history of neurological disease, major psychiatric disturbance, history of substance abuse, or psychoactive prescriptive medications usage. The protocol was approved by the local institutional review board, and written informed consent was obtained from all participants according to institutional guidelines at the University of New Mexico. No participants reported any adverse effects following exposure to cold stimuli in this study.

### Thermal Pain Stimulus Calibration and Tasks

Participants rested supine within a 3.0 Tesla Siemens Trio scanner with their head secured by a forehead strap, to limit head motion within the head coil. E-Prime software (Psychology Software Tools, Inc.) was used for stimulus presentation and synchronization of stimulus events with the MRI scanner. Visual stimuli were rear-projected using a Sharp XG-C50X LCD projector on an opaque white Plexiglas projection screen. A white visual fixation cross (visual angle = 1.02°) was presented on a black background throughout the course of the experiment to help participants maintain central fixation. At the start of the each run, a 0-to-10 scale appeared below the crosshair (visual eccentricity = 0.99°).

Cold pain stimuli were applied to the thenar surface of the right hand with an MRI-compatible thermode (30 × 30 mm, Pathway Model ATS system, MEDOC Advanced Medical Systems). Participants continuously rated their level of pain by pressing two buttons with their left hand that either increased or decreased the rating on the projected 0-to-10 Likert scale (0 = “No pain at all”, 10 = “Worst pain imaginable”). Current ratings were highlighted on the scale, and were updated at a frequency of 10 Hz to maintain temporal proximity between the button presses and changes on the screen.

Participants first completed an extensive calibration phase while they were in the MRI scanner to determine their subjective thresholds for low pain (rating of 3) and high pain (rating of 6; see Supplementary Methods section for detailed description of calibration procedures). The low pain task also served as a sensory control for the task as the only aspect that differed between the high and low pain stimulus was the temperature (i.e. intensity). A final destination temperature was determined for each subject for low and high pain conditions based on their subjective ratings during the calibration trials. The mean destination temperature across all subjects for the high pain condition was equal to 2.3 °C (standard deviation (SD) = 4.5 °C; range = 0 – 16 °C) and for the low pain condition was equal to 6.8 °C (SD = 6.4 °C; range = 0 – 20 °C). Notably, 4 individuals were assigned the same temperature for the low and high pain (0 °C) during calibration. Supplementary analyses indicated similar results with or without these participants (Figure S1). Therefore, data from these participants were retained to capture variance associated with ratings.

Following the calibration trial, participants continuously rated their level of pain during nine blocks of high and nine blocks of the low pain conditions. The thermode was in constant contact with the skin throughout the task, and was maintained at a baseline temperature of 32 °C before and after cold stimulus blocks. Each cold stimulus block consisted of an 8-second ramp-down to destination temperature, 16 seconds of cold stimulus maintained at destination temperature (individually determined in the calibration phase), and 6 seconds of ramp-up back to baseline temperature (32 °C). To account for the individual differences in the destination pain ratings and to maintain a similar experimental timeline across all subjects, the slope of temperature change in the ramp-down and ramp-up phase was predetermined and varied to account for differences in destination temperature. The inter-stimulus interval between subsequent cold stimuli varied in duration from 32 to 36 seconds to eliminate the development of temporal expectations regarding the start of the next trial. Three high and three low pain blocks were presented in a pseudo-randomized order within each run to minimize differential effects of habituation across the two conditions.

After completing the three runs of cold stimulus blocks, each subject performed a resting state task, in which they were asked to maintain fixation on a white crosshair for approximately 5 minutes.

## MR Imaging

High-resolution multi-echo T1 [TE (echo time) = 1.64, 3.5, 5.36, 7.22, 9.08 ms; TR (repetition time) = 2.53 s; 7° flip angle, number of excitations (NEX) = 1; slice thickness = 1 mm; FOV (field of view) = 256 mm; resolution = 256 × 256] anatomic images were collected at the beginning of each experiment. For the three pain fMRI series, 195 echo-

planar images were collected using a single-shot, gradient-echo echoplanar (EPI) pulse sequence [TR = 2000 ms; TE = 29 ms; flip angle = 75°; FOV = 240 mm; matrix size = 64 × 64]. Thirty-three contiguous sagittal 3.5-mm thick slices with a gap factor of 1.05 mm were selected to provide whole-brain coverage (voxel size: 3.75 × 3.75 × 4.55 mm) and to eliminate RF spillover effects on subsequent slices. An identical EPI pulse sequence was used to collect approximately 5 minutes of resting-state data for the functional connectivity analyses. For both functional experiments, the first image of each run was eliminated to account for T1 equilibrium effects in addition to two dummy scans.

### Image Processing and Statistical Analyses

For both task and resting state analyses, functional images were generated using Analysis of Functional NeuroImages (AFNI) software package (36). Time series images were spatially registered in both two- and three-dimensional space to the second EPI image of the first run to minimize effects of head motion, temporally interpolated to correct for slice-time acquisition differences and de-spiked. The resultant data were then transformed to a standard stereotaxic coordinate space (37) and spatially smoothed using a 6 mm Gaussian full-width half-maximum kernel.

For the task-based analyses, separate regressors for the low and high pain conditions were created by convolving the experimental time-course for each condition with a gamma variate function derived from known parameters of the hemodynamic response (38). Given the fixed experimental design, these two regressors were identical for all subjects and both will be referred to as ‘stimulus regressors’ throughout the paper. There were two additional regressors, which were tailored for each participant based on their individualized continuous pain ratings during all three runs of cold stimuli blocks. The ‘ratings regressor’ resembled a step function, with each button press signaling the onset of either increasing or decreasing subjective levels of pain (see Figure 1). This step function was then convolved with a gamma variate function based on the hemodynamic response, and reflected changes in subjective pain levels. The second regressor called the ‘button press regressor’ was modelled on effects associated with button presses as being transient in nature rather than a step function. Specifically, each button press was modeled as a single event and convolved with a gamma variate function (see Figure 1A). It was assumed that there would be correlation between the activation captured by the rating and button press models, but that the button press model would capture changes in the motor and visual system associated with the button press and the updating of the Likert scale on the screen (i.e., sensorimotor activation), as well as possible transient cognitive activity related to evaluating and rating the pain being experienced.

A voxel-wise multiple regression analysis was then used to estimate the beta weights corresponding to the two pain conditions, the motor response (button press regressor) and the individual subject’s pain rating (ratings regressor). Following this, a hierarchical multiple regression analysis was performed to isolate the unique variance associated with the ratings regressor (subjective pain) on a per subject basis. The incremental increases in variance ( $R^2$ ) captured by the addition of each successive regressor for the hierarchical regressions was calculated. The change in  $R^2$  was converted to a signed correlation

coefficient ( $r = \sqrt{R_2^2 - R_1^2} \times (\beta_2 / |\beta_2|)$ ) and then to a z-score using Fisher's method. For this analysis we entered the low pain stimulus regressor first, then the high pain stimulus regressor, then the motor regressor, and, last, the ratings regressor, with our ultimate goal being to isolate the unique variance associated with the subjective experience of pain, after removing the variance associated with both stimulus (high and low pain), and button press.

For the hierarchical regression results, one-sample t-tests were performed to identify the neuronal regions that exhibited variance for each of the individual regressors. A significance threshold corresponding to  $p < 0.005$  was applied in combination with a minimum cluster size threshold of 1663  $\mu\text{L}$  (26 native voxels) to all of the data to minimize the likelihood of false positives (39). The combination of these parameters resulted in a corrected alpha value of  $p < 0.05$  or below based on 10,000 Monte Carlo simulations.

For the resting state connectivity analyses, a regression analysis was conducted on individual subject's time-series to remove potential sources of noise (physiological and machine-based) from the data (40). First, individual anatomical images (i.e., T1) were segmented into maps of white matter, gray matter and cerebrospinal fluid (CSF) using FSL's FAST algorithm (41). Second, the resultant CSF and white matter masks were used to obtain an average time-series for these tissues during the extended resting state runs for each individual. Finally, all six movement parameters, the ROI-based time-series for CSF, the ROI-based time-series for white matter, a constant term, and a linear term were entered into a linear regression against the extended resting state time-series to remove the variance associated with each of these variables (40).

The connectivity seeds were derived from regions showing significant activation during subjective pain (ratings regressor). Coordinates for connectivity seeds were chosen such that the entire volume of the seed fully resided in areas of significant activation, and, wherever possible, to be in and around maxima in these areas. Resting-state time courses were then averaged for each empirically derived seed (in the case of unilateral seeds) or seeds (in the case of bilateral seeds), which were then used as the primary regressor for the whole-brain functional connectivity analyses. The resultant correlation coefficients were then converted to z-scores using Fisher's method.

For the connectivity analyses, one-sample t-tests were performed to identify regions of functional connectivity. A significance threshold corresponding to  $p < 0.0001$  was applied in combination with a minimum cluster size threshold of 960  $\mu\text{L}$  (15 native voxels) to all of the data to minimize the likelihood of false positives (39). The combination of these parameters resulted in a corrected alpha value of  $p < 0.005$  or below based on 10,000 Monte Carlo simulations.

## Results

### Behavioral Results

A  $2 \times 9$  [Intensity (high, low) x Order (1<sup>st</sup> through 9<sup>th</sup> block)] repeated-measures ANOVA was performed on mean pain ratings during stimulus periods to examine differences between perceived pain levels at the two stimulus intensities, and to evaluate the potential



effects of habituation. Results indicated significant main effects of intensity ( $F_{1,19} = 25.61$ ,  $p < 0.001$ ), with condition means suggesting higher pain ratings in the high (mean rating =  $1.78 \pm 1.04$ ) relative to the low (mean rating =  $1.08 \pm 0.73$ ) pain condition (Figure 2). There was a significant main effect of order ( $F_{4,81,91.41} = 5.21$ ,  $p < 0.01$ ), but the intensity  $\times$  order interaction effect was not significant ( $p > 0.10$ ). To further investigate the effects of order, mean ratings for both high and low pain blocks were averaged across each of the functional imaging runs (each run contained 3 high and 3 low pain blocks) and compared in a pair-wise fashion. The results indicated that pain ratings were significantly higher in the first run (mean =  $1.57 \pm 0.83$ ) compared to both the second (mean =  $1.42 \pm 0.77$ ;  $t_{19} = 2.46$ ,  $p = 0.02$ ) and the third (mean =  $1.32 \pm 0.75$ ;  $t_{19} = 3.94$ ,  $p < 0.01$ ) runs. There was trend towards a difference between the second and third runs ( $t_{19} = 1.86$ ,  $p = 0.08$ ). Only one participant rated the high pain stimulus as 0, and only in 2 out of the 9 blocks.

Pain ratings during the baseline periods (32–36 second inter-stimulus intervals) following cold-stimulus applications were analyzed in a similar manner. The  $2 \times 9$  [Baseline (high, low)  $\times$  Order (1<sup>st</sup> through 9<sup>th</sup> rest block)] repeated-measures ANOVA indicated a significant main effect of intensity of preceding pain block ( $F_{1,19} = 19.26$ ,  $p < 0.01$ ), with significantly higher ratings during baseline periods following high pain blocks (mean rating =  $0.86 \pm 0.74$ ) compared to low pain blocks (mean rating =  $0.33 \pm 0.37$ ). There was a significant main effect of order ( $F_{3,07,58.41} = 2.86$ ,  $p = 0.04$ ), and an interaction effect that trended towards significance ( $F_{2,39,58.41} = 2.44$ ,  $p = 0.09$ ). To follow up the interaction, simple effects testing suggested that the difference was greatest during rest block 1 ( $t_{19} = 5.90$ ,  $p < 0.01$ ). Similarly, pain ratings were significantly lower in the rest periods of the third run (mean =  $0.49 \pm 0.11$ ) compared to both the first (mean =  $0.63 \pm 0.17$ ;  $t_{19} = 2.72$ ,  $p = 0.01$ ) and the second (mean =  $0.67 \pm 0.17$ ;  $t_{19} = 2.16$ ,  $p = 0.04$ ) runs.

### Correlation of Regressors

In the next set of analyses the correlations amongst the four individual regressors, low pain, high pain, ratings, and button press, were evaluated on a subject-wise basis. For each potential relationship, the number of subjects who exhibited a statistically significant ( $p < 0.05$ ) correlation between the regressors was tabulated (see Table 1). In addition, the mean, standard deviation, minimum and maximum correlations for each of the pairwise comparisons across all subjects are reported when applicable. Results indicated that regressors were significantly correlated with each other for the majority of subjects, with the exception of the low pain versus both the ratings and button press regressors. As expected the correlation between the ratings and button press regressors was the highest. However, there was considerable variability in the relationship between stimulus and ratings regressors (Table 1). For example, some subjects' ratings tended to closely coincide with the onset of painful stimuli (Figure 1B, Subjects 1 and 4), whereas other subjects showed temporal dissociation between stimulus onset and pain ratings (i.e., continued pain after discontinuation of cold stimulus, Figure 1B, Subject 2) or rated subjective pain levels around 0 during both conditions (Figure 1B, Subject 3).

## Functional Results: Hierarchical Regression Analyses

The low pain condition was entered into the hierarchical regression first, and was associated with broad areas of deactivation in several regions that have been previously associated with the default-mode network (DMN) (40, 42–44) including the bilateral medial PFC/ventral ACC [Brodmann Areas (BAs) 9,10,11,24,32,47], superior frontal gyrus (BA 8), medial temporal lobes (BAs 28,35), inferior temporal cortex (BAs 21,22,37,38), IPL (BA 40) and PCC (BAs 23,30). Negative activation was also observed within the bilateral insula, auditory (BAs 41,42), visual (BAs 18,19), primary somatosensory (BA 3) and motor cortices (BA 4) and cerebellum, as well as within the bilateral striatum and thalamus. Additional areas of negative activation unique to the left hemisphere were located in the dorsolateral prefrontal cortex (DLPFC) extending to premotor cortex (BAs 6,8,9,46) and left angular gyrus (BA 39). There were no regions that were associated with a positive activation during the low pain condition.

The high pain condition was uniquely associated with similar regions of deactivation as the low pain condition. In addition, areas of positive activation included the bilateral anterior insula, bilateral dACC extending into the pre-SMA (BAs 6,8,24,32) and the right lateral prefrontal cortex (PFC) including ventrolateral prefrontal cortex (VLPFC) and DLPFC (BAs 9,10,44,45,46,47). Additional areas of positive activation included the right inferior parietal lobule (IPL) and superior parietal lobule (SPL) (BAs 7,40), thalamus, striatum, and globus pallidus (Figure 3).

The motor regressor resulted in positive activation within all areas of the pain neuromatrix including bilateral somatosensory cortex (BAs 1,2,3), IPL and SPL (BAs 5,39,40) including S1 and S2, precuneus (BA7), anterior and posterior insula (BA 13), lateral and medial PFC (BAs 9,10,44,45,46,47), dACC and middle cingulate cortex (MCC) (24,32), temporal cortex (BAs 20,22,36,37,38,41,42), bilateral visual cortex (BAs 17,18,19) and PCC (BAs 23,31). As expected, there was activation throughout the bilateral premotor and motor cortex (BAs 4,6,8), cerebellum, thalamus, and striatum. There was some additional negative activation in the DMN including bilateral medial PFC (BAs 10,11,24,25,32), left PCC and precuneus (BA 7,23,30,31), left temporal cortex (BA 36,39) and right temporal cortex (BA 21), as well as left premotor cortex (BA 8).

The ratings regressor was associated with unique variance and more extensive activation in similar regions as high pain regressor (see Figure 3). Results indicated increased activation in the bilateral anterior insula extending into posterior VLPFC (BAs 44,47), lateral PFC including VLPFC and DLPFC (right greater than left; BAs 6,8,9,10,45), ACC extending into preSMA and SMA (right greater than left; BAs 6,8,32), and inferior and superior parietal lobules (BAs 7,39,40) extending into R precuneus (BAs 7,19). Finally, there was activation observed in the right striatum and thalamus and in the left cerebellum. The ratings regressor also identified unique variance in similar clusters of the DMN as the high pain condition (deactivation), although to a lesser extent (Figure 3). There was additional deactivation located in the bilateral premotor, motor and sensory cortices (BAs 3,4,6).



## Functional Results: Functional Connectivity Analyses

Empirically derived seed regions for the connectivity analyses were determined from the hierarchical multiple regression analyses based on the results from the ratings regressor (Figure 3). Specifically, the R dACC (coordinates = 8,23,32), bilateral anterior insula (coordinates = +/- 32,20,4), R medial thalamus (coordinates = 10,-9,6), and R DLPFC (coordinates = 37,27,33) were each selected as four separate seed regions (9 mm diameter spheres, center of mass coordinates in Talairach space) to be used in the connectivity analyses. See supplemental results (Figure S2) for seed locations.

The results from this analysis are summarized in Figure 4 and 5. In brief, anterior insula demonstrated connectivity with S2, posterior insula (sensory/discriminative), dACC, medial thalamus (affective/motivational), DLPFC, IPL (cognitive/evaluative) and preSMA/SMA (motor). Medial thalamus demonstrated connectivity with anterior insula, and dACC (affective motivational). dACC demonstrated connectivity with anterior insula, medial thalamus (affective/motivational), DLPFC, IPL (cognitive/evaluative), and preSMA and SMA (motor). DLPFC demonstrated connectivity with anterior insula, dACC (affective/motivational), IPL (cognitive/evaluative), preSMA and SMA (motor).

## Discussion

The current study utilized hierarchical multiple regression to isolate the variance in brain activation associated with subjective pain experience during a noxious cold stimulus. Behavioral findings provide evidence of the subjective nature of pain based on a temporal mis-match between stimulus delivery and subjective pain ratings. Moreover, increases and decreases in pain ratings were temporally disjoint from the cold stimuli to varying degrees between subjects, often persisting into rest periods. Habituation further contributed to response variability with significant decreases in pain ratings from the first and second runs to the final run of the experimental paradigm. Not surprisingly, as a result of this high degree of variability in pain sensation and rating, our ratings regressor, reflecting the subjective experience of pain, captured more areas of brain activity and additional unique variance within the pain network, presumably as a result of a better match to the temporal dynamics of the *subjective* cold pain experience relative to the stimulus regressor.

Although we had expected the low pain condition to be associated with some positive activation in the pain network, as previous work has demonstrated that near-noxious stimuli evoke activation in the pain network (insula, thalamus, dACC, PFC, striatum, S1, S2) (45), we only saw deactivation in this condition, and this was likely due to the stimulus being too weak (mean individual rating = 1.08). In fact, we also observed deactivation in some of the pain regions during the low pain stimulus (insula, thalamus, somatosensory cortex). This may have occurred because anticipation of pain causes activation in some of these same regions (45), and so, when individuals realized during the low pain condition that they would not receive the high pain stimulus, the resolution of anticipation may have resulted in deactivation in these regions. During both the low and high pain stimulus, the default mode network was also deactivated, as has been seen in previous work (23), and this likely occurred because the DMN deactivates during tasks. The high pain regressor was also found to be associated with activation in a number of areas of the brain that have previously been

shown to respond to other kinds of near-noxious and painful stimuli, including the bilateral dACC, pre-SMA, anterior insula, thalamus and the right DLPFC and VLPFC (3, 5, 6, 23, 45). Importantly, the average maximum rating for the high pain was also relatively low in spite of our extensive calibration efforts, with a mean individual rating of 1.97.

After accounting for the variance associated with the low pain, high pain and button press regressors with the hierarchical regression, the ratings regressor captured unique variance within a variety of brain regions, including anterior insula, and extending into other areas commonly reported to be part of the pain response network including dorsal ACC, thalamus and DLPFC. These regions are likely the primary brain regions involved in processing the subjective experience of pain for a variety of stimuli (1–3, 5, 7, 11, 21, 23, 24). Our findings demonstrated that using continuous ratings and a percept model for investigations of pain-related brain activation may be better able to capture variance associated with subjective pain than stimulus-based models. This may be particularly true in cases where habituation or temporal dissociation between stimulus onset and subjective experience exists, or where high pain stimuli are only mildly painful (as was true in our study).

Previous work regarding the recruitment of anterior versus posterior insula during the subjective experience of pain has been mixed, with some studies finding that posterior insula alone is associated with the experience of subjective pain (21, 46), and others implicating both anterior and posterior insula (2). Our findings indicate that activation in anterior, but not posterior, insula is associated with subjective pain. Activation in posterior insula may not have been present in our work due to the fact that posterior insula may be deactivated during ratings of subjective pain levels (47). Interestingly, a region of negative activation in the rostral/subgenual ACC was also uniquely captured by the ratings regressor (Figure 3). This region has been implicated as a part of the endogenous pain inhibition circuitry and habituation (48, 49) and a negative correlation between activation in this area and subjective pain ratings may have been related to the habituation in subjective pain levels seen in our study.

Neither S1 nor S2 were activated by our high pain or ratings regressors, which was somewhat unexpected, as these are a major projection sites for ascending sensory nerve bundles. Historically, the role of S1 in processing pain has been controversial; human pain imaging studies have shown mixed results in S1, activation in this area may not be strongly related to subjective reports of pain (1, 7, 50, 51), and it may play a larger role in encoding localization and thermal information rather than pain (51–53). Conflicting findings for S1 have been attributed to a variety of factors including task variability (eg. effects of attention, stimulus timing and intensity) (50), mixed inhibitory and excitatory effects of nociceptive input to this area, and inadequate spatial resolution of human imaging techniques (excitatory effects may be in small focal areas), although limited spatial resolution appears to play less and less of a role as techniques improve (1, 7, 50, 53). Human hemodynamic imaging studies have also shown mixed results for S2, although its role in processing pain is less controversial than S1 (1). Of note, however, both S1 and S2 were captured by the button press regressor. By putting the button press regressor, which was highly correlated with the ratings regressor, into the model before the ratings regressor, we may have lost variance associated with ratings to the button press regressor. It is also possible that we did not see S1

and S2 activation because the pain stimuli were not salient enough to detect a signal in these relatively small corresponding regions.

Cold pain may be different in temporal pattern, afferent fiber activation, and perceived qualitative characteristics from other types of pain (26, 27). Individuals with pain syndromes like fibromyalgia may also respond differently to cold versus heat pain in terms of habituation versus sensitization; both fibromyalgia patients and healthy controls habituate to heat pain, but individuals with fibromyalgia sensitize to cold pain and controls habituate (16). Despite these differences, previous work, using stimulus-based models, have found that the neural matrix associated with cold pain stimuli in healthy individuals is similar to that associated with heat pain, and is associated with activation in ACC, insula, MCC, S2, DLPFC, VLPFC, premotor cortex, striatum, thalamus, PAG (3, 18, 27, 54). Our study, which to our knowledge is the first to investigate the brain activation associated with continuous ratings during cold pain, also demonstrated similar regions of activation as other continuous ratings studies using heat pain. Our results provide a starting point for further work into the aberrant processing of cold pain in syndromes like fibromyalgia.

Previous work posits the existence of up to four important sub-networks which process the subjective experience of pain (1, 3, 11). One may be related to emotional aspects of processing painful stimuli, which is often associated with activation in dorsal ACC, anterior insula (3, 7, 24, 55–58) and medial thalamus (3, 7, 55, 59, 60). Another proposed network is involved in the cognitive aspects of processing painful stimuli, and top-down modulation of pain perception (61, 62), and includes the DLPFC and IPL, regions mediating a wide range of attentional, cognitive, and inhibitory processes (7). A third is described as the sensory/discriminative network, including the ventroposterolateral (VPL) thalamus, S1, S2, other sensory areas, and posterior insula (3, 7, 11, 63). A fourth is the motor network which is comprised of preSMA, SMA (3) and MCC (64). In addition to being named as part of the affective/motivational network, the dACC has also been posited to integrate information about affect, cognition, and response selection during pain processing (11). The insula has been theorized to carry somatosensory information from regions such as S2, which is a primary projection site for ascending pain neurons, to regions involved in assigning emotional salience to pain stimuli (1, 11)

Functional connectivity analyses were used to examine co-occurring fluctuations within other brain regions using seeds from regions which were activated by the ratings regressor in order to further explore the validity of such models. Our results supported the posited roles of dACC and insula as key relay sites during neural processing of subjective pain. First, in our analyses the dACC demonstrated connectivity with regions posited to comprise the affective/motivational network (anterior insula and medial thalamus), the cognitive/evaluative network (DLPFC, IPL), and the motor network (preSMA, and SMA), supporting its theorized role as an integrator. Moreover, of the seeds tested, only the anterior insula demonstrated connectivity with posterior insula and S2, (both involved in sensory/discriminative aspects of pain processing), and it also demonstrated connectivity with regions involved in the affective response to pain (dACC and medial thalamus) and cognitive/evaluative regions (IPL and DLPFC), indicating that anterior insula may be

essential for linking regions involved in processing sensory/discriminative information with regions involved in assigning cognitive and emotional salience to stimuli.

There are several limitations to the current study. First, because participants rated their pain continuously, we were unable to fully isolate brain activation associated with the subjective experience of pain (ratings regressor) from the experience of rating one's own subjective pain levels (button press regressor). Previous work suggests that the motor and cognitive components of subjective rating are associated with activation in many of the same regions involved in processing painful stimuli, including premotor and motor cortex, SMA, striatum, thalamus, cerebellum, parietal cortex, and DLPFC (65, 66) and insula and ACC (67). Another disadvantage of obtaining ratings in real-time is that the act of rating one's own pain increases activity in regions implicated in the pain network (21, 47) which could explain some of the unusually large positive effects we saw in our study. However, by entering the button press regressor prior to entering the ratings regressor, we likely removed the majority of variance related to the motor components, and some of the variance related to the cognitive components of rating. Moreover, it has been argued that the continuous, as opposed to episodic, ratings of pain minimize extraneous brain activity such as that associated with episodic memory and error detection (21), and capturing subjective ratings in real-time allowed for us to capture variance associated with subjective pain during non-stimulus epochs. Therefore, there are both advantages and disadvantages to using continuous ratings as we did.

Another limitation is that we did not attain target ratings of 6 and 3, and that there was only a small (but still significant) difference in terms of mean pain rating between high and low pain, which could have partially explained why the ratings regressor captured significantly more pain-related brain activation compared to the stimulus regressor. The presence of such a small difference in ratings could have been related to habituation, which was observed to occur throughout the scanner session. Moreover, four of the subjects had the same high and low pain temperatures, as a result of our calibration process. However, despite the fact that the differences in ratings between high and low pain stimuli were less pronounced than we expected, we still observed unique variance associated with high pain, above and beyond that which was observed with low pain. Moreover, a hierarchical regression was more conservative than a standard regression would have been, as a greater amount of variance was attributed to the stimulus regressors, although the results for the ratings regressor would have been identical for both models (see Figure S1 for side-by-side comparison between the results for a hierarchical regression and for a standard regression). More specifically, a hierarchical regression attributes both common and unique variance to regressors entered earlier (high pain regressor) in the regression, and only unique variance to regressors entered last in the regression (ratings regressor). That the ratings regressor still captured more positive activation than the high pain regressor despite this conservative approach emphasizes the utility of percept-related models to identify brain networks involved in processing pain.

In summary, the results of the current study provide further information about the brain networks responsible for the experience of subjective pain, and demonstrate the utility of percept-models during studies of central processing of pain. These findings can help guide

future studies, and focus investigations to particular anatomical regions. Future work using percept-based models of continuous ratings in chronic pain patients, investigating both evoked and spontaneous pain in the context of pharmacological or behavioral interventions, should be done, and could give added insight into how the subjective pain experience and its neural correlates is altered in this condition and possible targets for future treatment interventions.

## Supplementary Material

Refer to Web version on PubMed Central for supplementary material.

## Acknowledgments

This work was supported by the National Institutes of Health [1 R03 DA022435 to A.M.; K23 AA021156 to C.W]. Special thanks to Diana South and Cathy Smith for assistance with data collection.

## References

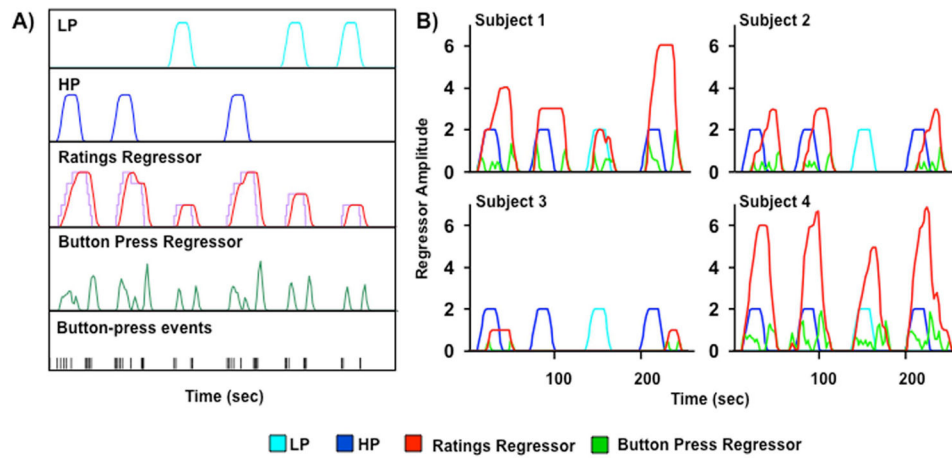
1. Apkarian AV, Bushnell MC, Treede RD, Zubieta JK. Human brain mechanisms of pain perception and regulation in health and disease. *Eur J Pain*. 2005; 9:463–84. [PubMed: 15979027]
2. Wager TD, Atlas LY, Lindquist MA, Roy M, Woo CW, Kross E. An fMRI-based neurologic signature of physical pain. *N Engl J Med*. 2013; 368:1388–97. [PubMed: 23574118]
3. Davis KD, Moayedi M. Central mechanisms of pain revealed through functional and structural MRI. *J Neuroimmune Pharmacol*. 2012; 8:518–34. [PubMed: 22825710]
4. Duerden EG, Albanese MC. Localization of pain-related brain activation: a meta-analysis of neuroimaging data. *Hum Brain Mapp*. 2013; 34:109–49. [PubMed: 22131304]
5. Porro CA, Baraldi P, Pagnoni G, Serafini M, Facchin P, Maieron M, et al. Does anticipation of pain affect cortical nociceptive systems? *J Neurosci*. 2002; 22:3206–14. [PubMed: 11943821]
6. Porro CA, Cettolo V, Francescato MP, Baraldi P. Temporal and intensity coding of pain in human cortex. *J Neurophysiol*. 1998; 80:3312–20. [PubMed: 9862924]
7. Peyron R, Laurent B, Garcia-Larrea L. Functional imaging of brain responses to pain. A review and meta-analysis (2000). *Neurophysiol Clin*. 2000; 30:263–88. [PubMed: 11126640]
8. Tracey I. Imaging pain. *Br J Anaesth*. 2008; 101:32–9. [PubMed: 18556697]
9. Tracey I, Ploghaus A, Gati JS, Clare S, Smith S, Menon RS, et al. Imaging attentional modulation of pain in the periaqueductal gray in humans. *J Neurosci*. 2002; 22:2748–52. [PubMed: 11923440]
10. Moisset X, Bouhassira D. Brain imaging of neuropathic pain. *Neuroimage*. 2007; 37 (Suppl 1):S80–8. [PubMed: 17512757]
11. Schnitzler A, Ploner M. Neurophysiology and functional neuroanatomy of pain perception. *J Clin Neurophysiol*. 2000; 17:592–603. [PubMed: 11151977]
12. Mouraux A, Diukova A, Lee MC, Wise RG, Iannetti GD. A multisensory investigation of the functional significance of the “pain matrix”. *Neuroimage*. 2011; 54:2237–49. [PubMed: 20932917]
13. Davis KD. Neuroimaging of pain. *Suppl Clin Neurophysiol*. 2004; 57:72–7. [PubMed: 16106607]
14. Chen JI, Ha B, Bushnell MC, Pike B, Duncan GH. Differentiating noxious- and innocuous-related activation of human somatosensory cortices using temporal analysis of fMRI. *J Neurophysiol*. 2002; 88:464–74. [PubMed: 12091568]
15. Condes-Lara M, Calvo JM, Fernandez-Guardiola A. Habituation to bearable experimental pain elicited by tooth pulp electrical stimulation. *Pain*. 1981; 11:185–200. [PubMed: 7322602]
16. Smith BW, Tooley EM, Montague EQ, Robinson AE, Cospser CJ, Mullins PG. Habituation and sensitization to heat and cold pain in women with fibromyalgia and healthy controls. *Pain*. 2008; 140:420–8. [PubMed: 18947923]

17. Ernst M, Lee MH, Dworkin B, Zaretsky HH. Pain perception decrement produced through repeated stimulation. *Pain*. 1986; 26:221–31. [PubMed: 3763235]
18. Davis KD, Pope GE, Crawley AP, Mikulis DJ. Neural correlates of prickle sensation: a percept-related fMRI study. *Nat Neurosci*. 2002; 5:1121–2. [PubMed: 12368810]
19. Apkarian AV, Krauss BR, Fredrickson BE, Szeverenyi NM. Imaging the pain of low back pain: functional magnetic resonance imaging in combination with monitoring subjective pain perception allows the study of clinical pain states. *Neurosci Lett*. 2001; 299:57–60. [PubMed: 11166937]
20. Baliki MN, Chialvo DR, Geha PY, Levy RM, Harden RN, Parrish TB, et al. Chronic pain and the emotional brain: specific brain activity associated with spontaneous fluctuations of intensity of chronic back pain. *J Neurosci*. 2006; 26:12165–73. [PubMed: 17122041]
21. Baliki MN, Geha PY, Apkarian AV. Parsing pain perception between nociceptive representation and magnitude estimation. *J Neurophysiol*. 2009; 101:875–87. [PubMed: 19073802]
22. Kwan CL, Diamant NE, Pope G, Mikula K, Mikulis DJ, Davis KD. Abnormal forebrain activity in functional bowel disorder patients with chronic pain. *Neurology*. 2005; 65:1268–77. [PubMed: 16247056]
23. Lui F, Duzzi D, Corradini M, Serafini M, Baraldi P, Porro CA. Touch or pain? Spatio-temporal patterns of cortical fMRI activity following brief mechanical stimuli. *Pain*. 2008; 138:362–74. [PubMed: 18313223]
24. Kong J, White NS, Kwong KK, Vangel MG, Rosman IS, Gracely RH, et al. Using fMRI to dissociate sensory encoding from cognitive evaluation of heat pain intensity. *Hum Brain Mapp*. 2006; 27:715–21. [PubMed: 16342273]
25. Corradi-Dell'Acqua C, Hofstetter C, Vuilleumier P. Felt and seen pain evoke the same local patterns of cortical activity in insular and cingulate cortex. *J Neurosci*. 2011; 31:17996–8006. [PubMed: 22159113]
26. Simone DA, Kajander KC. Excitation of rat cutaneous nociceptors by noxious cold. *Neurosci Lett*. 1996; 213:53–6. [PubMed: 8844711]
27. Seifert F, Maihofner C. Representation of cold allodynia in the human brain--a functional MRI study. *Neuroimage*. 2007; 35:1168–80. [PubMed: 17360197]
28. Taylor KS, Seminowicz DA, Davis KD. Two systems of resting state connectivity between the insula and cingulate cortex. *Hum Brain Mapp*. 2009; 30:2731–45. [PubMed: 19072897]
29. Craggs JG, Price DD, Verne GN, Perlstein WM, Robinson MM. Functional brain interactions that serve cognitive-affective processing during pain and placebo analgesia. *Neuroimage*. 2007; 38:720–9. [PubMed: 17904390]
30. Zaki J, Ochsner KN, Hanelin J, Wager TD, Mackey SC. Different circuits for different pain: patterns of functional connectivity reveal distinct networks for processing pain in self and others. *Soc Neurosci*. 2007; 2:276–91. [PubMed: 18633819]
31. Malinen S, Vartiainen N, Hlushchuk Y, Koskinen M, Ramkumar P, Forss N, et al. Aberrant temporal and spatial brain activity during rest in patients with chronic pain. *Proc Natl Acad Sci U S A*. 2010; 107:6493–7. [PubMed: 20308545]
32. Kluetsch RC, Schmahl C, Niedtfeld I, Densmore M, Calhoun VD, Daniels J, et al. Alterations in default mode network connectivity during pain processing in borderline personality disorder. *Arch Gen Psychiatry*. 2012; 69:993–1002. [PubMed: 22637967]
33. Baliki MN, Geha PY, Apkarian AV, Chialvo DR. Beyond feeling: chronic pain hurts the brain, disrupting the default-mode network dynamics. *J Neurosci*. 2008; 28:1398–403. [PubMed: 18256259]
34. Ploner M, Lee MC, Wiech K, Bingel U, Tracey I. Prestimulus functional connectivity determines pain perception in humans. *Proc Natl Acad Sci U S A*. 2010; 107:355–60. [PubMed: 19948949]
35. Mayer AR, Franco AR, Ling J, Canive JM. Assessment and quantification of head motion in neuropsychiatric functional imaging research as applied to schizophrenia. *J Int Neuropsychol Soc*. 2007; 13:839–45. [PubMed: 17697415]
36. Cox RW. AFNI: software for analysis and visualization of functional magnetic resonance neuroimages. *Comput Biomed Res*. 1996; 29:162–73. [PubMed: 8812068]



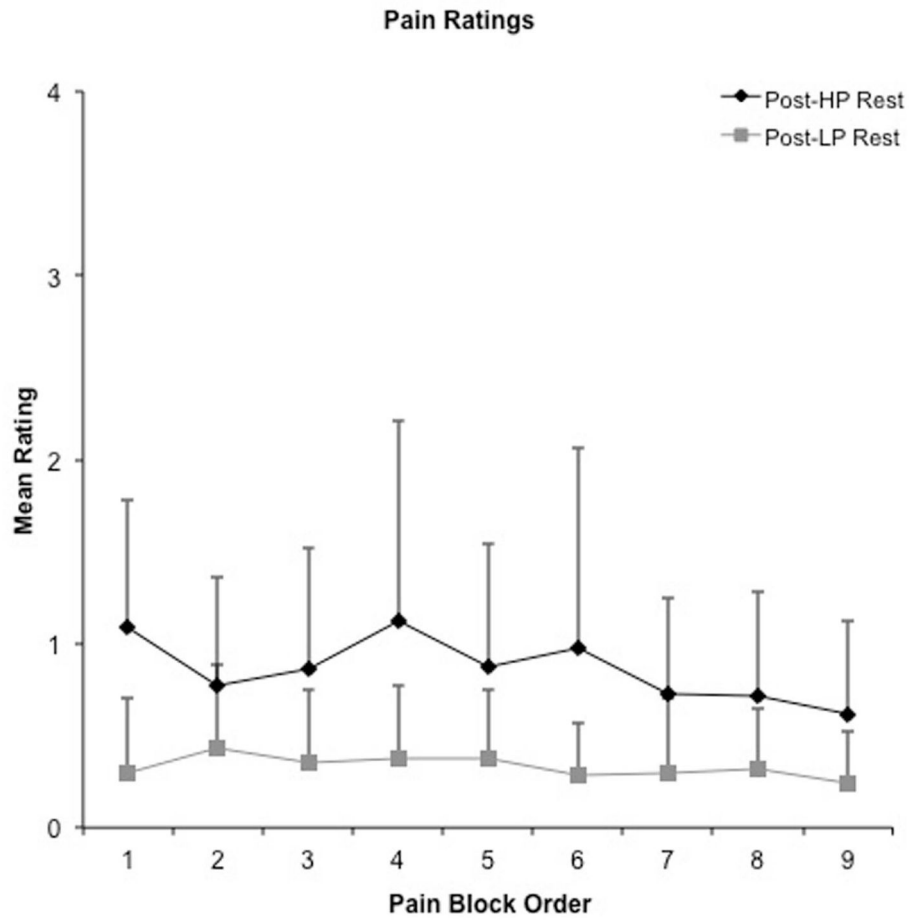
37. Talairach, J.; Tournoux, P. Co-planar Stereotaxic Atlas of the Human Brain: 3-Dimensional Proportional System - an Approach to Cerebral Imaging. New York: Thieme Medical Publishers; 1988.
38. Cohen HL, Porjesz B, Begleiter H, Wang W. Neurophysiological correlates of response production and inhibition in alcoholics. *Alcohol Clin Exp Res.* 1997; 21:1398–406. [PubMed: 9394110]
39. Forman SD, Cohen JD, Fitzgerald M, Eddy WF, Mintun MA, Noll DC. Improved assessment of significant activation in functional magnetic resonance imaging (fMRI): use of a cluster-size threshold. *Magn Reson Med.* 1995; 33:636–47. [PubMed: 7596267]
40. Fox MD, Snyder AZ, Vincent JL, Corbetta M, Van Essen DC, Raichle ME. The human brain is intrinsically organized into dynamic, anticorrelated functional networks. *Proc Natl Acad Sci U S A.* 2005; 102:9673–8. [PubMed: 15976020]
41. Zhang Y, Brady M, Smith S. Segmentation of brain MR images through a hidden Markov random field model and the expectation-maximization algorithm. *IEEE Trans Med Imaging.* 2001; 20:45–57. [PubMed: 11293691]
42. Fransson P. Spontaneous low-frequency BOLD signal fluctuations: an fMRI investigation of the resting-state default mode of brain function hypothesis. *Hum Brain Mapp.* 2005; 26:15–29. [PubMed: 15852468]
43. Buckner RL, Andrews-Hanna JR, Schacter DL. The brain's default network: anatomy, function, and relevance to disease. *Ann N Y Acad Sci.* 2008; 1124:1–38. [PubMed: 18400922]
44. Raichle ME, MacLeod AM, Snyder AZ, Powers WJ, Gusnard DA, Shulman GL. A default mode of brain function. *Proc Natl Acad Sci U S A.* 2001; 98:676–82. [PubMed: 11209064]
45. Brodersen KH, Wiech K, Lomakina EI, Lin CS, Buhmann JM, Bingel U, et al. Decoding the perception of pain from fMRI using multivariate pattern analysis. *Neuroimage.* 2012; 63:1162–70. [PubMed: 22922369]
46. Oertel BG, Preibisch C, Martin T, Walter C, Gamer M, Deichmann R, et al. Separating brain processing of pain from that of stimulus intensity. *Hum Brain Mapp.* 2012; 33:883–94. [PubMed: 21681856]
47. Schoedel AL, Zimmermann K, Handwerker HO, Forster C. The influence of simultaneous ratings on cortical BOLD effects during painful and non-painful stimulation. *Pain.* 2008; 135:131–41. [PubMed: 17611034]
48. Mobascher A, Brinkmeyer J, Warbrick T, Musso F, Schlemper V, Wittsack HJ, et al. Brain activation patterns underlying fast habituation to painful laser stimuli. *Int J Psychophysiol.* 2010; 75:16–24. [PubMed: 19833154]
49. Bingel U, Schoell E, Herken W, Buchel C, May A. Habituation to painful stimulation involves the antinociceptive system. *Pain.* 2007; 131:21–30. [PubMed: 17258858]
50. Bushnell MC, Duncan GH, Hofbauer RK, Ha B, Chen JI, Carrier B. Pain perception: is there a role for primary somatosensory cortex? *Proc Natl Acad Sci U S A.* 1999; 96:7705–9. [PubMed: 10393884]
51. Vierck CJ, Whitsel BL, Favorov OV, Brown AW, Tommerdahl M. Role of primary somatosensory cortex in the coding of pain. *Pain.* 2013; 154:334–44. [PubMed: 23245864]
52. Moulton EA, Pendse G, Becerra LR, Borsook D. BOLD responses in somatosensory cortices better reflect heat sensation than pain. *J Neurosci.* 2012; 32:6024–31. [PubMed: 22539862]
53. Frot M, Magnin M, Mauguiere F, Garcia-Larrea L. Cortical representation of pain in primary sensory-motor areas (S1/M1)--a study using intracortical recordings in humans. *Hum Brain Mapp.* 2013; 34:2655–68. [PubMed: 22706963]
54. Casey KL, Minoshima S, Morrow TJ, Koeppe RA. Comparison of human cerebral activation pattern during cutaneous warmth, heat pain, and deep cold pain. *J Neurophysiol.* 1996; 76:571–81. [PubMed: 8836245]
55. Vogt BA. Pain and emotion interactions in subregions of the cingulate gyrus. *Nat Rev Neurosci.* 2005; 6:533–44. [PubMed: 15995724]
56. Brooks JC, Nurmikko TJ, Bimson WE, Singh KD, Roberts N. fMRI of thermal pain: effects of stimulus laterality and attention. *Neuroimage.* 2002; 15:293–301. [PubMed: 11798266]
57. Singer T, Seymour B, O'Doherty J, Kaube H, Dolan RJ, Frith CD. Empathy for pain involves the affective but not sensory components of pain. *Science.* 2004; 303:1157–62. [PubMed: 14976305]

58. Lin CS, Hsieh JC, Yeh TC, Lee SY, Niddam DM. Functional dissociation within insular cortex: the effect of pre-stimulus anxiety on pain. *Brain Res.* 2013; 1493:40–7. [PubMed: 23200718]
59. Lane RD, Waldstein SR, Chesney MA, Jennings JR, Lovallo WR, Kozel PJ, et al. The rebirth of neuroscience in psychosomatic medicine, Part I: historical context, methods, and relevant basic science. *Psychosom Med.* 2009; 71:117–34. [PubMed: 19196808]
60. Treede RD, Kenshalo DR, Gracely RH, Jones AK. The cortical representation of pain. *Pain.* 1999; 79:105–11. [PubMed: 10068155]
61. Lorenz J, Minoshima S, Casey KL. Keeping pain out of mind: the role of the dorsolateral prefrontal cortex in pain modulation. *Brain.* 2003; 126:1079–91. [PubMed: 12690048]
62. Apkarian AV. Cortical pathophysiology of chronic pain. *Novartis Found Symp.* 2004; 261:239–45. discussion 45–61. [PubMed: 15469054]
63. Ab Aziz CB, Ahmad AH. The role of the thalamus in modulating pain. *The Malaysian journal of medical sciences: MJMS.* 2006; 13:11–8. [PubMed: 22589599]
64. Vogt BA, Derbyshire S, Jones AK. Pain processing in four regions of human cingulate cortex localized with co-registered PET and MR imaging. *Eur J Neurosci.* 1996; 8:1461–73. [PubMed: 8758953]
65. Mattay VS, Callicott JH, Bertolino A, Santha AK, Van Horn JD, Tallent KA, et al. Hemispheric control of motor function: a whole brain echo planar fMRI study. *Psychiatry Res.* 1998; 83:7–22. [PubMed: 9754701]
66. Gountouna VE, Job DE, McIntosh AM, Moorhead TW, Lymer GK, Whalley HC, et al. Functional Magnetic Resonance Imaging (fMRI) reproducibility and variance components across visits and scanning sites with a finger tapping task. *Neuroimage.* 2010; 49:552–60. [PubMed: 19631757]
67. Hutcherson CA, Goldin PR, Ochsner KN, Gabrieli JD, Barrett LF, Gross JJ. Attention and emotion: does rating emotion alter neural responses to amusing and sad films? *Neuroimage.* 2005; 27:656–68. [PubMed: 15946863]



**Figure 1.**

Panel A depicts sample regressor models. Low (LP; cyan) and high (HP; blue) pain regressors are based on stimulus delivery parameters (onset, duration time). Ratings regressor (red) is modeled on subject's continuous ratings of pain (purple) convolved with a gamma variate function based on hemodynamic response. Button press regressor (green) is modeled on button press events, convolved with a gamma variate function. Panel B depicts representative graphs for four different subjects plotting the four regressors used in the two hierarchical models. Subjects 1 and 2 demonstrate the expected differentiation in pain ratings (red) between high pain (blue) and low pain (cyan) stimulus blocks, with subject 2 also showing a temporal dissociation between stimulus and ratings onset times. Subject 3 rated all pain stimuli as close to 0 on the Likert scale, while Subject 4 rated all pain stimuli at greater than 5. Button press regressor (green) shows button press event timing.



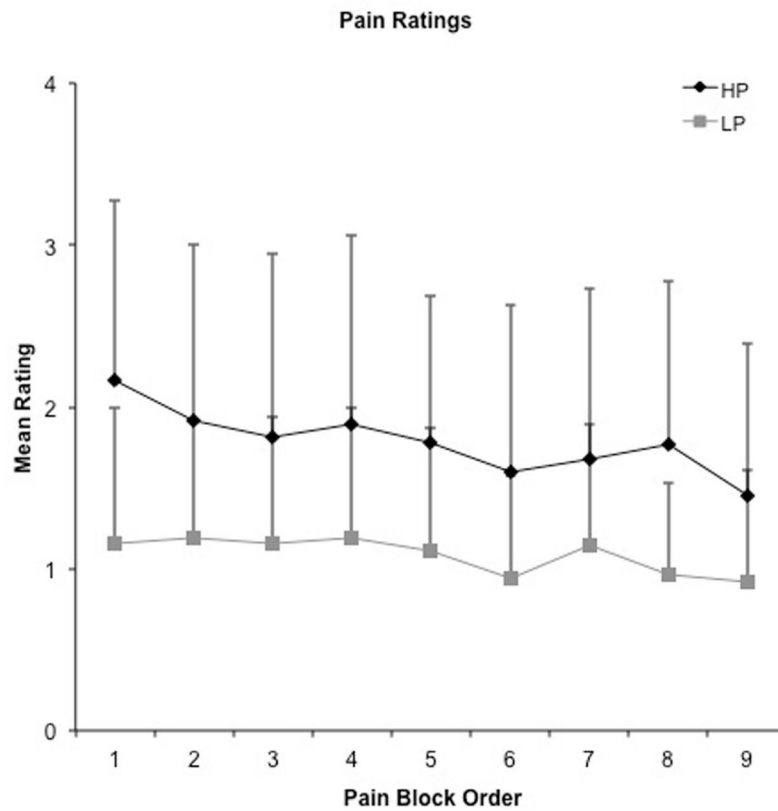


**Figure 2.** Mean pain ratings as a function of rest (Top) and pain stimulus (Panel B, gray symbols) blocks. Rest blocks (inter-stimulus intervals) followed all stimulus blocks. Both post high pain block ratings (Post-HP) and high pain ratings (H) (black diamonds) were significantly higher than post low pain block ratings (Post-LP) and low pain ratings (LP) (grey squares) for both rest and pain blocks.

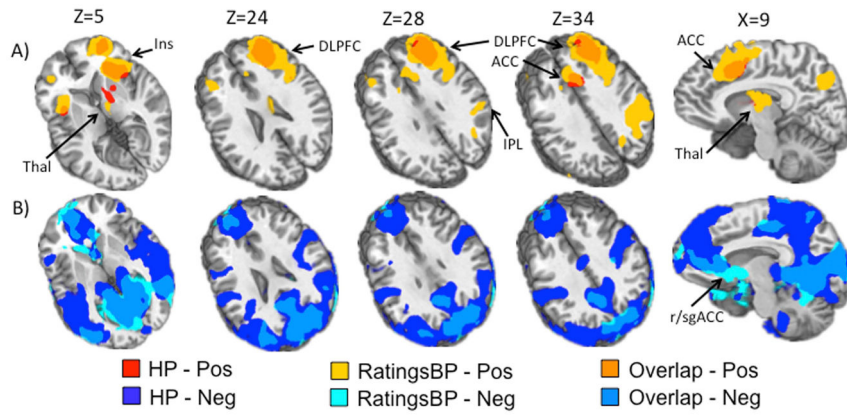


**Figure 3.**

This figure presents the results for the high pain regressor and the ratings regressor from the hierarchical regression where regressors were entered in the following order from first to last: low pain, high pain, button press, ratings. Of note the ratings regressor captured more extensive and unique positive activation above and beyond that of the high pain regressor. Panel A (top) shows areas of unique variance associated with the high pain regressor (HP; red), the ratings regressor after correcting for variance associated with the button press regressor (RatingsBP) (yellow), and overlap between the two (orange). Panel B (bottom) shows areas of unique variance associated with HP (dark blue), RatingsBP (light blue) and Overlap (medium blue). Regions indicated by arrows include 1) insula (Ins); 2) thalamus (Thal); 3) anterior cingulate cortex (ACC); 4) dorsolateral prefrontal cortex (DLPFC); 5) inferior parietal lobule (IPL); 6) rostral/subgenual ACC (r/sgACC). Slice locations (Z) are given according to the Talairach atlas.



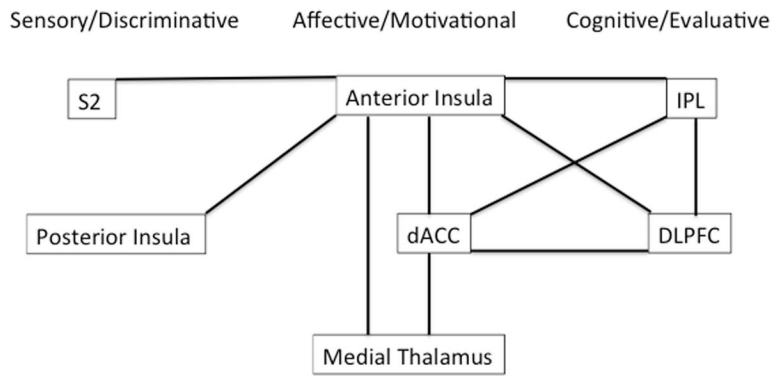


**Figure 4.** This figure simplistically depicts the results from the connectivity analyses. It organizes regions into groups according to models which propose central pain-processing networks to be comprised of at least four distinct subnetworks: a sensory/discriminative network, an affective/motivational network, a cognitive evaluative network, and a motor network (not depicted in this figure). Black lines connect regions which were significantly positively correlated with one another (demonstrated connectivity) in our analyses. (S2: secondary somatosensory cortex, dACC: dorsal anterior cingulate cortex, DLPFC: dorsolateral prefrontal cortex, IPL: inferior parietal lobule).

Author Manuscript

Author Manuscript

Author Manuscript

Author Manuscript

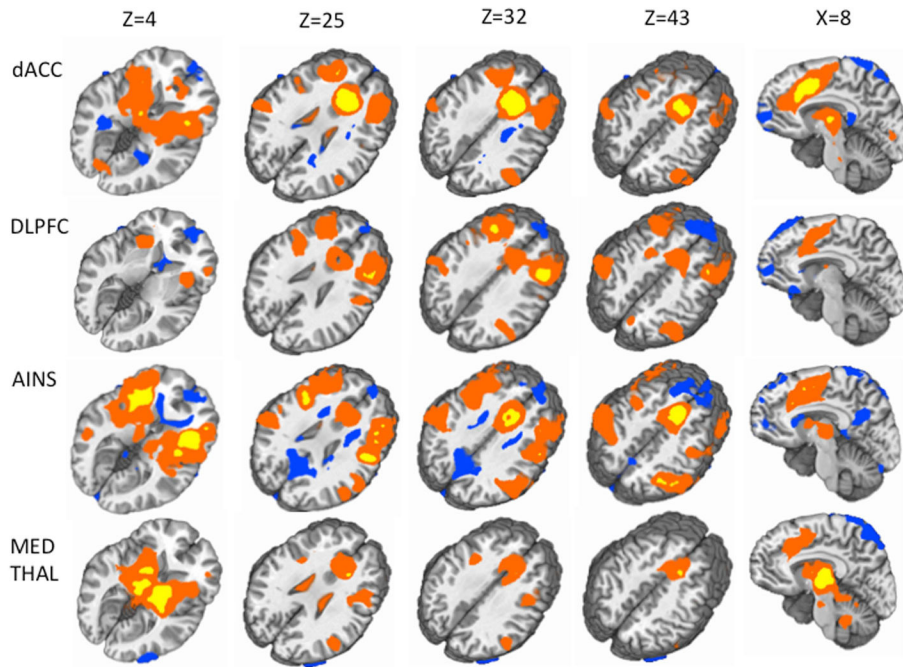


**Figure 5.**

This figure depicts the results from the connectivity analyses. Each row indicates the results for a different seed (from top to bottom: right dACC, right DLPFC, bilateral anterior insula, right medial thalamus). Each column represents a different slice location according to the Talairach atlas (from left to right:  $Z=4$ ,  $Z=25$ ,  $Z=43$ ,  $X=8$ ). Areas which were significantly positively correlated with seeds (positive  $Z$  scores) are displayed in this figure in either yellow (Fischer's  $Z > 10$ ) or red (Fischer's  $Z < -10$ ). Areas which were significantly negatively correlated with seeds (negative  $Z$  scores) are displayed in blue (Fischer's  $Z < -10$ ).

**Table 1**

Descriptive summary of the correlations between regressors for all subjects

	N *	Mean r	SD	MIN	MAX
Low Pain – High Pain	20	-0.2312	N/A **	N/A **	N/A **
Low Pain - Ratings	12	0.0480	0.1713	-0.2810	0.4472
High Pain - Ratings	16	0.2873	0.2139	-0.1407	0.7651
Low Pain – Button Press	8	0.0203	0.0854	-0.1554	0.1909
High Pain – Button Press	17	0.1762	0.0823	-0.0098	0.3323
Ratings – Button Press	20	0.3696	0.1466	0.1180	0.6782

\* Number of subjects (maximum = 20) whose regressors show a significant correlation at  $p < .05$ .

\*\* Due to fixed experimental conditions there was no variation across subjects for these two regressors.